Results of the 2014 UT modeling benchmark obtained with models implemented in CIVA

Sylvain Chatillon, Sebastien Robert, Philippe Bredif, Pierre Calmon, Guillaume Daniel, Francois Cartier

Results of the 2014 UT Modeling Benchmark Obtained with Models Implemented in CIVA
Solution of the FMC-TFM Ultrasonic Benchmark Problem Using CIVA

Sylvain Chatillon, Sébastien Robert, Philippe Brédif, Pierre Calmon,

Guillaume Daniel and François Cartier

CEA, LIST, 91191Gif-sur-Yvette, France

Abstract. The last decade has seen the emergence of new ultrasonic array techniques going beyond the simple application of suitable delays (phased array techniques) for focusing purposes. Amongst these techniques, the particular method combining the so-called FMC (Full Matrix Capture) acquisition scheme with the synthetic focusing algorithm denoted by TFM (Total Focusing Method) has become popular in the NDE community. The 2014 WFNDEC ultrasonic benchmark aims at providing FMC experimental data for evaluating the ability of models to predict images obtained by TFM algorithms (or equivalent ones). In this paper we describe the benchmark and report comparisons obtained with the CIVA simulation software. The simulations and measurements are carried out on two steel blocks, one in carbon steel and another in stainless steel. The reference probe is a 64 elements linear array, with .5mm element width and a gap of .1mm, working at 5 MHz. The benchmark problem consists in predicting images of vertical and tilted notches located on plane or inclined backwalls. The notches have different heights and different ligaments. The images can be obtained considering different paths (direct echoes or corner echoes). For each notch, the full matrix capture (FMC) have been recorded in one unique position with the probe positioned such that than angle between the probe axis and the notch direction corresponds to 45°. The results are calibrated on the response of a 2mm side drilled hole. For each case, TFM images have been reconstructed for both experimental and simulated signals. The models used are those implemented in CIVA based on Kirchhoff approximation. Comparisons are reported and discussed.

Keywords: Ultrasonic Benchmark, Phased Array Probe, UT Simulation, Kirchhoff, SOV
PACS: 43.35.Yb

INTRODUCTION

For several years, the World Federation of NDE center, WFNDEC, proposes benchmark study in which simulated results (in either ultrasonic, X-rays or eddy current NDT configurations) obtained with various models are compared to experiments.

The Total Focusing Method (TFM) is an advanced post-processing imaging algorithm of ultrasonic array data. It can be performed using several propagation modes (direct or over skip imaging) and several types of waves (longitudinal or transverse). This method shows great potential in defect detection and characterization. In particular, it allows the imaging of extended defects. This imaging technique is more and more used and is now implemented in acquisition systems. Moreover, the simulation of the Full Matrix Capture (FMC) acquisition enables the prediction of the reconstructed images, including artefacts, and thus provides tools for image analyze and inspection optimization.

This year, the UT benchmark has been proposed to evaluate the ability of the models to simulate the FMC acquisitions and to reproduce the TFM images. The computations presented in this paper were performed using the version CIVA 11. In the future, this experimental data could be also used to compare several processing algorithms.

DESCRIPTION OF THE 2014 ULTRASONIC BENCHMARK

For a complete description of the studied configurations, see [2]. The measurements were performed on 2 steel mock-ups. The first one is planar, made of carbon steel 1020 and containing several embedded and backwall breaking notches of different heights (Figures 1 and 2). The second one, made of stainless steel 302, exhibits inclined backwalls with several slopes and contains several backwall breaking notches of different heights (Figure 3). In addition, each mock-up contains a 2 mm diameter side drilled hole, embedded at the same depth as the rectangular defects, to provide a reference echo.

A 64 elements linear contact phased-array probe was used (Figure 4). The element width is 0.5 mm and the gap between elements is 0.1 mm, corresponding to a whole aperture of 38.3mm and 10mm respectively in the incident and orthogonal directions.

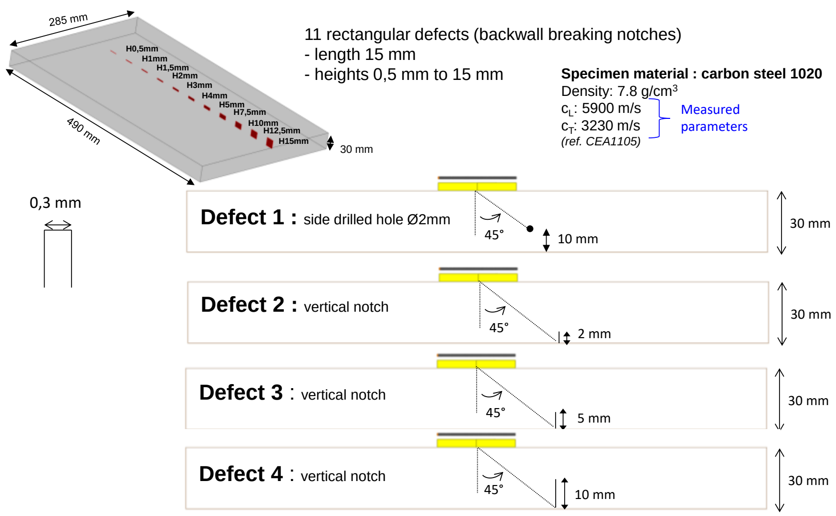

FIGURE 1. Description of the first Mock-up and defects implemented inside.

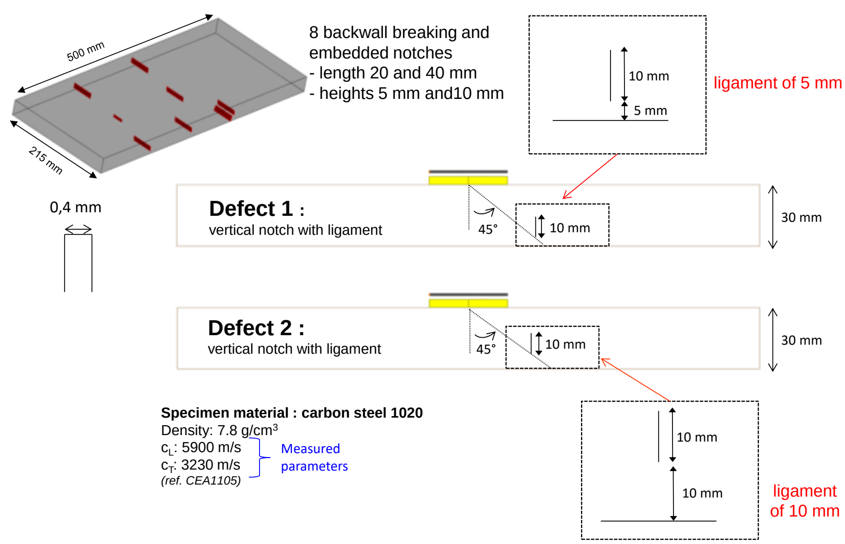

FIGURE 2. Description of the second Mock-up and defects implemented inside.

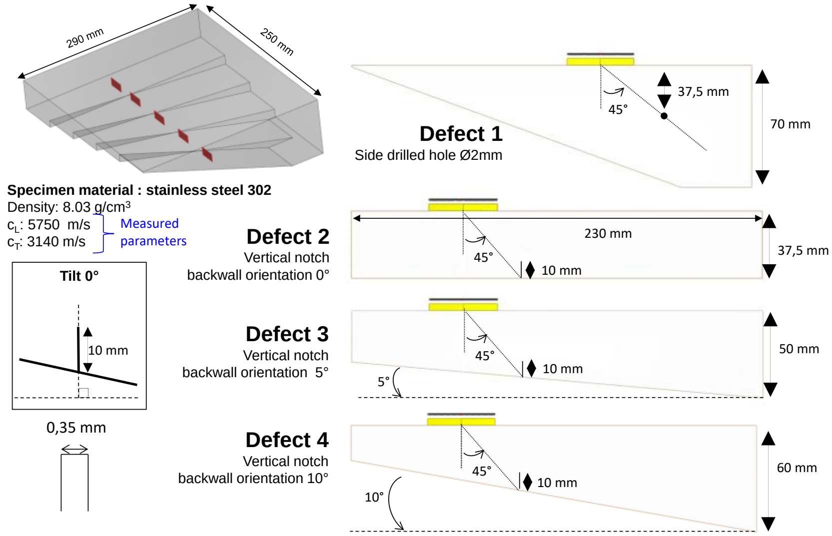

FIGURE 3. Description of the third Mock-up and defects implemented inside

The TFM imaging is a technique used to post-process the data from Full Matrix Capture (FMC)[3,6]. For an ultrasonic array of N elements, the FMC acquisition consists in recording a set of NxN elementary signals $S_{ij}(t)$, where (i, j) is a transmit and receive element combination, $1 \leq i,j \leq N$. The post-processing algorithm consists then in coherently summing all the acquired data at every point in a given Region Of Interest (ROI), so that an image of this region can be produced which shows maximum of intensity where the scattering target (the defect) is located. Mathematically the algorithm in its simpliest form can be expressed as:

$$I(P)=\sum_{i,j=1}^{N} S_{ij}\left[t_{ij}(P)\right] \tag{1}$$

where $t_{ij}(P)$ denotes the theoretical time of flight corresponding to the propagation time between the i-th transmitter and the j-th receiver, through the point P.

The TFM imaging can be performed considering one or another wave path (direct or after backwall reflection) and several types of waves (longitudinal or transverse) [5,6]. For over skip imaging, the theoretical times of flight in (1) include ray paths with one or more reflections at the backwall, while for direct imaging, the considered ray paths do not contain any backwall reflection. This TFM imaging is implemented in the CIVA software and offers three commonly used imaging modes shown in Figure 1: direct, corner echo and indirect imaging.

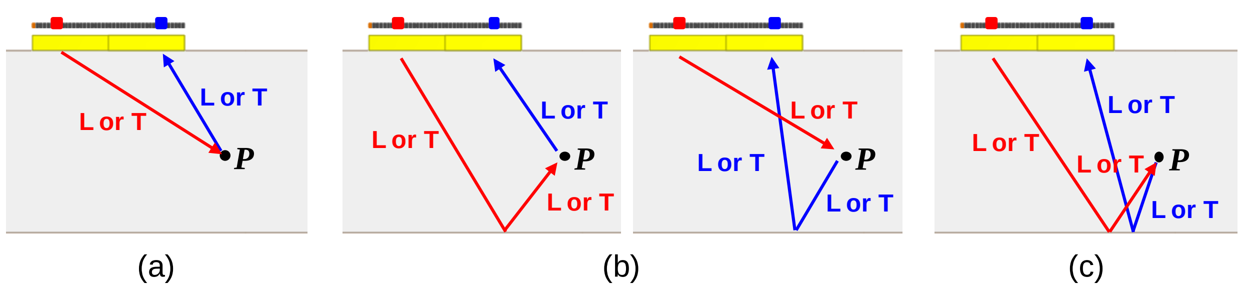

FIGURE 4. Scheme of the different TFM imaging modes: a) direct imaging, b) corner echo imaging, c) indirect imaging.

A review of the models implemented in Civa for field and echo computations can be found in [7].

For this study, the amplitudes of the side drilled holes were calculated with the SOV model of echo-defect interaction while the Kirchhoff/GTD model [8], [9] was used for the calculation of the notches echoes. All the echoes computations were performed with CIVA release 11.

EXPERIMENTAL VALIDATION PROCEDURE

The experimental validation process has been done following the recommendations of ref [10]. To describe the realistic configurations in CIVA, experimental measurements of some parameters were performed.
Regarding the specimen, the longitudinal (L) and transverse (T) waves velocities (V_L and V_T) have been estimated by measuring the time between successive backwall echoes. The velocities used for the computation in CIVA are V_L=5900m/s and V_T=3230m/s. The uncertainty of the velocity measurement has been evaluated to ± 30 m/s.
The material homogeneity has also been checked by comparing the maximum of amplitude of the backwall echo measured at several positions of the probe. A 0.5dB maximal dispersion over all probe positions has been obtained (figure5). Concerning the probe, the sensitivity measurement has confirmed that there was no dead element and the dispersion over the 64 elements was less than 3dB (Figure 6).

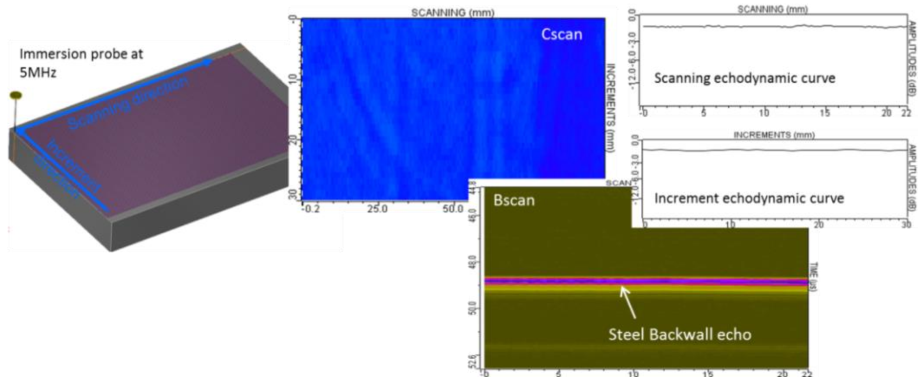

FIGURE 5. . Example of experimental material homogeneity check. Cscan with a backwall echo storage.

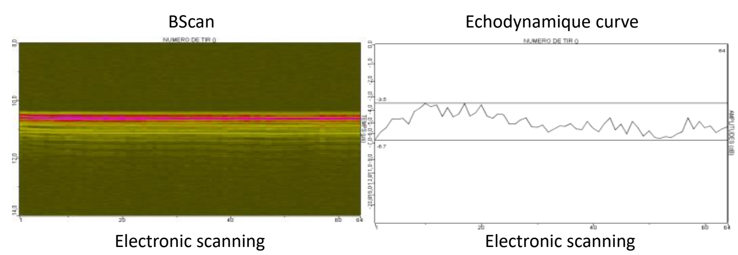

FIGURE 6. Sensitivity measurement on backwall echo in ferritic steel.

RESULTS ON THE FIRST BLOCK : PLANAR BACKWALL

First, we have compared the simulated and experimental TFM images obtained on the SDH embedded at 30mm depth (figure 7). We can observe a very good agreement between the two images in terms of echo position, shape and size. The maximum of the amplitude on this SDH images have been used in order to calibrate the comparisons between experimental and simulated notches images. In this section we report the comparisons performed on the notches in the two planar blocks. It is important to notice that, for the simulations, we have taken into account the opening of the notch (values given by the manufacturer) to accurately simulate the diffraction echoes. Examples of comparisons are given on figures 8, 9, 10 and 11 for direct and corner echo modes, including mode conversions.

In all cases, a very good agreement between simulated and experimental images can be observed. All the echoes, including the tip diffraction echoes, the corner echoes and even the artifacts, are correctly predicted. The location, the shape and the size are well reproduced by the simulation and the maximal amplitude discrepancy is less than 3dB. These images illustrates the great potential offered by the TFM algorithm applied to corner echoes for imaging extended defects.

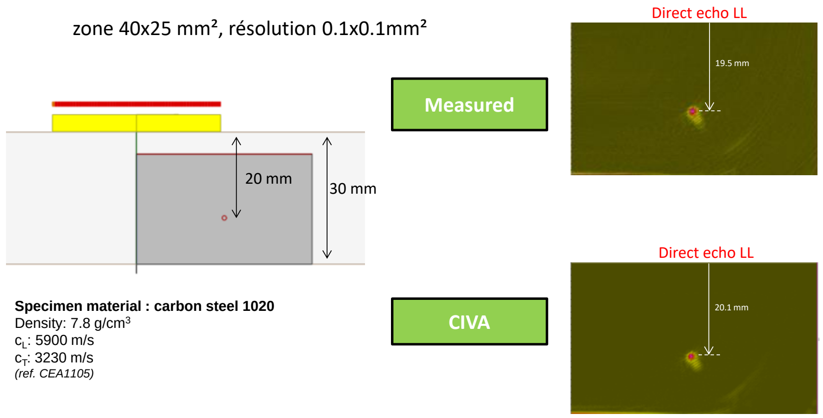

FIGURE 7. Simulated and experimental TFM images obtained on the 2mm SDH at 30 mm depth.

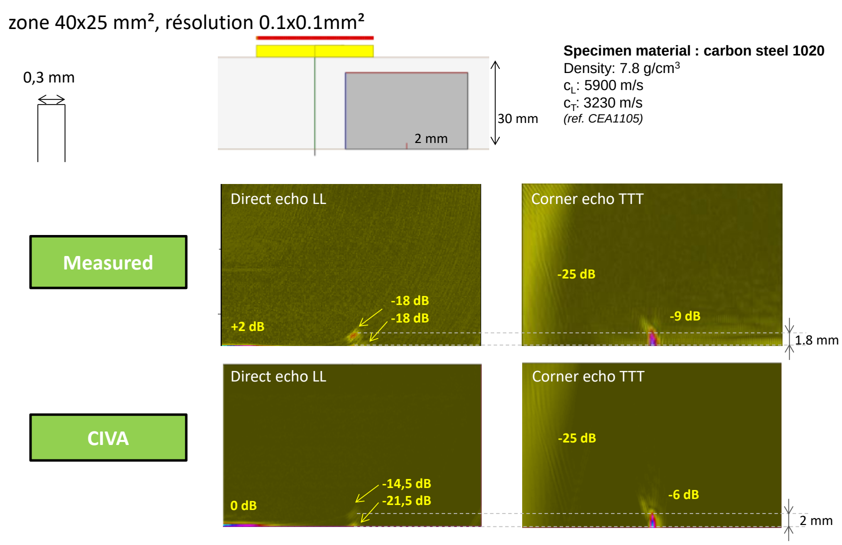

FIGURE 8. simulated and experimental TFM images obtained on the 2mm height backwall breaking notch.

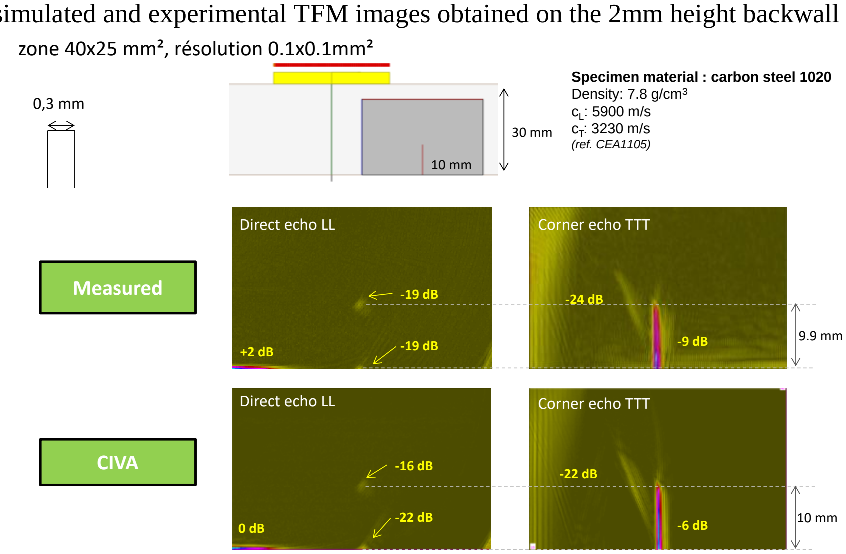

FIGURE 9. simulated and experimental TFM images obtained on the 10mm height backwall breaking notch.

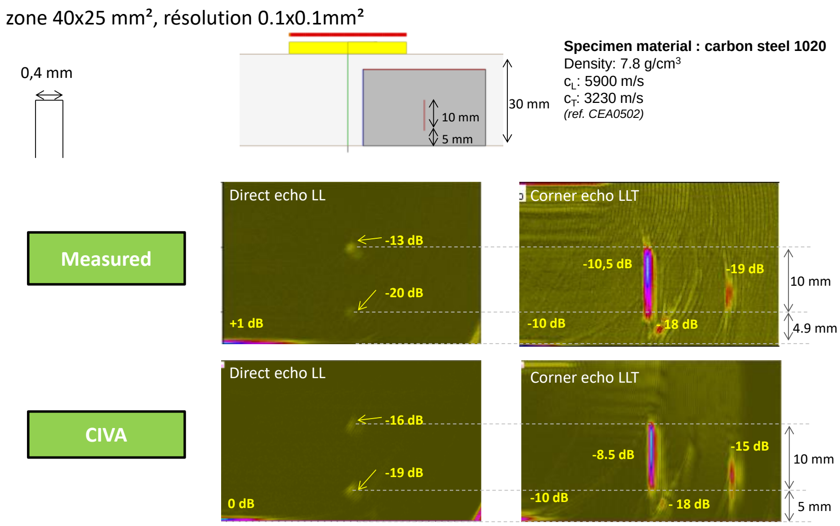

FIGURE 10. simulated and experimental TFM images obtained on the 10mm height embedded notch with 5 mm ligament

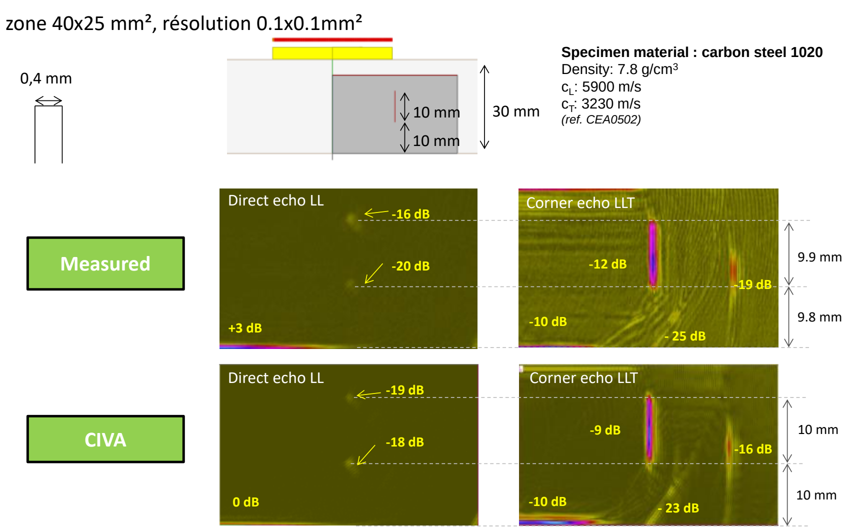

FIGURE 11. simulated and experimental TFM images obtained on the 10mm height embedded notch with 10 mm ligament

RESULTS ON THE SECOND BLOCK : INCLINED BACKWALL

In the same way, we have firstly compared the TFM images obtained on the 2mm side drilled hole embedded at 37.5 mm depth. The results are displayed on figure 12. Once again, we can observe a very good agreement between the both, in terms of echo position, shape and size. The amplitude of the experimental and simulated echoes again will be used as references to compare the amplitude of the notches responses.

The same comparisons have been performed on the 10 mm height backwall breaking notches located on several slopes. Examples of comparisons are given on figures 13, 14 and 15 for direct and corner echo modes, including mode conversions. Once again, in all cases, a very good agreement between simulated and experimental images can be observed. All the echoes, including the tip diffraction echoes, the corner echoes and even the artifacts, are correctly predicted. The location, the shape and the size are well reproduced by the simulation. Once again, the agreement between experimental and simulated amplitude are less than 3 dB, excepted in one case, corresponding to the mixed corner echo mode, for which the discrepancy is 6dB. This disagreement has to be investigated, but it doesn’t seem to be due to the inclined backwall, since the same discrepancy is observed on the planar part of the same block (figure 13). In particular, the hypothesis of isotropy of the block has to checked.

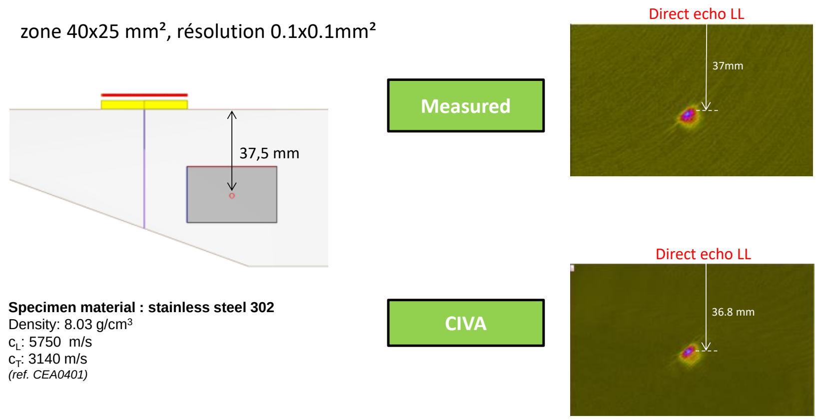

FIGURE 12. simulated and experimental TFM images obtained on the 2mm SDH at 37.5 mm depth.

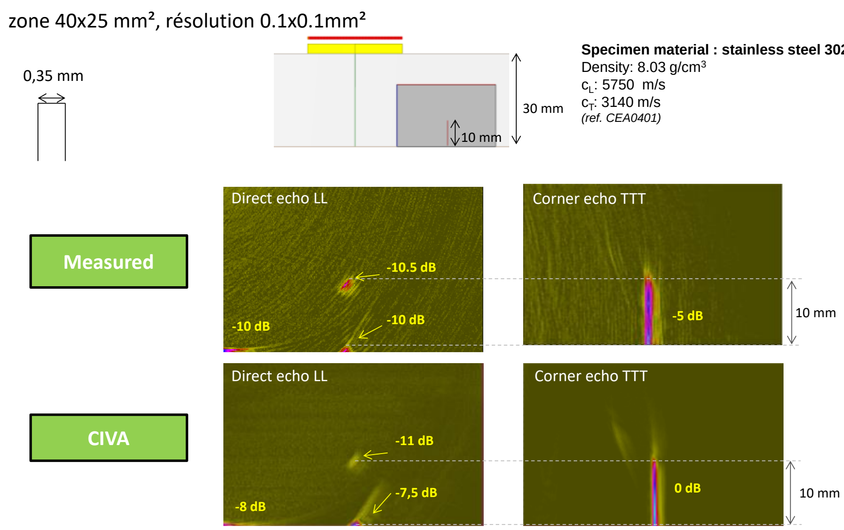

FIGURE 13. simulated and experimental TFM images obtained on the 10mm height notch with the 0° slope.

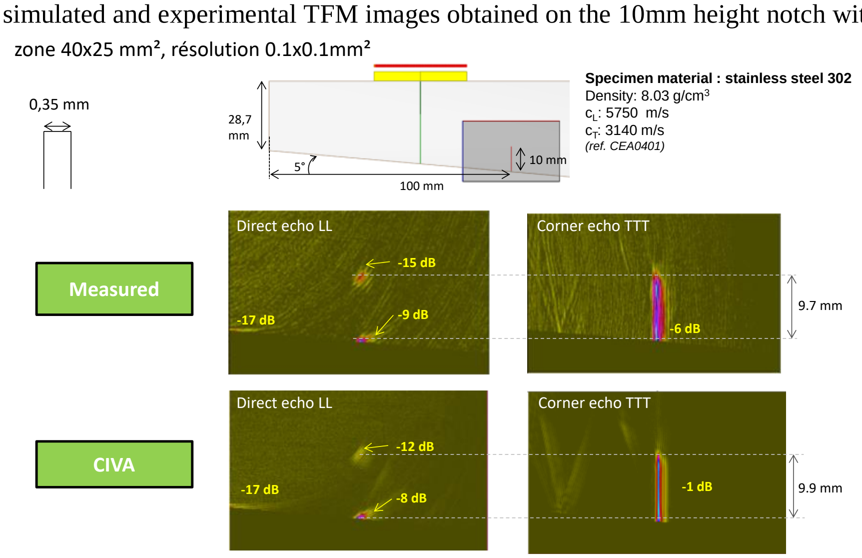

FIGURE 14. simulated and experimental TFM images obtained on the 10mm height notch with the 5° slope.

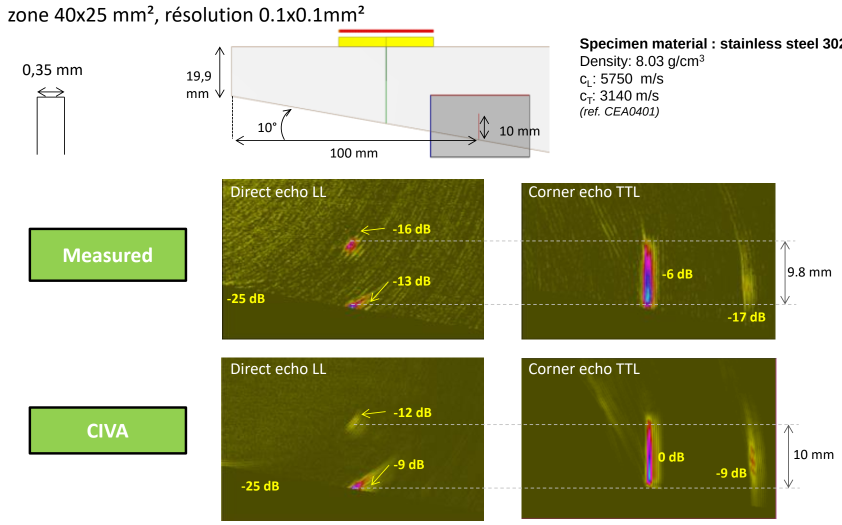

FIGURE 15. simulated and experimental TFM images obtained on the 10mm height notch with the 10° slope.

CONCLUSION

This WFNDEC 2014 UT benchmark is dedicated to FMC acquisitions and TFM processing. Acquisitions have been carried out on several steel blocks containing embedded and backwall breaking notches and side drilled holes. The aim of this paper was to evaluate the ability of CIVA UT module to reproduce the FMC acquisitions and multi-mode TFM images. Multi-modes reconstructions were applied on experimental and simulated data to obtain edge diffraction and corner echoes, with or without mode conversion. In all cases, the experimental and simulated images are in very good agreement. All the echoes, including tip diffraction, corner with or without mode conversion, and even artifacts, are correctly predicted in terms of location, shape and size. The general agreement in amplitude, calibrated on side drilled holes, is less than 3 dB, except for one case which is under investigation. This later has to be investigated. These results highlight the ability of the simulation to provide efficient tools to predict, analyze and optimize inspection configurations using FMC and TFM. One perspective might be now to use these UT benchmark experimental data for evaluating different imaging algorithms.

REFERENCES

1. More details and references may be found on http://www-civa.cea.fr.
2. 2013 Ultrasonic benchmarks, http://www.wfndec.org/benchmarkproblemscurrent.htm.
3. C. Holmes, B.W. Drinkwater, P.D. Wilcox, “Post-processing of the full matrix of ultrasonic transmit-receive array data for non-destructive evaluation”, NDT&E international, Vol. 38, pp. 701-711, 2005.
4. P. Calmon, E. Iakovleva, A. Fidahoussen, G. Ribay, S. Chatillon, “ Model based reconstruction of UT array data”, in Review in progress in QNDE, vol 27, 699, (2008)
5. A. Fidahoussen, P. Calmon, M. Lambert, S. Paillard, S. Chatillon, “Imaging of defects in several complex configurations by simulation-helped processing of ultrasonic array data”, Review of progress in QNDE, Vol. 29, pp. 847-854, 2009.
6. J. Zhang, B.W. Drinkwater, P.D. Wilcox, A.J. Hunter, “Defect detection using ultrasonic arrays: The multi-mode total focusing method”, NDT&E international, Vol. 43, pp. 123-133, 2010.
7. S. Mahaut, M. Darmon, S. Chatillon, F. Jenson and P. Calmon, "Recent advances and current trends of ultrasonic modelling in CIVA", Insight, 51(2), (2009).
8. V. Dorval, M. Darmon S. Chatillon and L. Fradkin, "Prediction of the ultrasonic response of crack-like defects using a mixed Kirchhoff-GTD model", in this proceedings.
9. L. Schmerr and S-J. Song Ultrasonic Non destructive Evaluation Systemes, Springer, p. 241–258, 2007
10. Recommendations for the use and validation of NDT simulation, V, IIW Best practice document, IIW 2363-13(2013).